Supplementary Information

Robust metal–organic framework monoliths for long-cycling lithium metal batteries

Chaejeong Kim[‡a], *Wooyoung Jeong*[‡b], *Hong Rim Shin*[a], *Kyu-Nam Jung*[*c], *Jong-Won Lee*[*a]

[a] Division of Materials Science and Engineering, Hanyang University, 222 Wangsimni-ro, Seongdong-gu, Seoul 04763, Republic of Korea

[b] Department of Energy Science and Engineering, Daegu Gyeongbuk Institute of Science and Technology (DGIST), 333 Techno Jungang-daero, Hyeonpung-eup, Dalseong-gun, Daegu 42988, Republic of Korea

[c] Renewable Energy Institute, Korea Institute of Energy Research (KIER), 152 Gajeong-ro, Yuseong-gu, Daejeon 34129, Republic of Korea

[‡] These authors contributed equally to this work.

[*] Corresponding authors.

E-mail addresses: mitamire@kier.re.kr (K.-N. Jung), jongwonlee@hanyang.ac.kr (J.-W. Lee)

Supplementary note 1 Experimental details on the liquid adsorption test

The porosity of the membrane was calculated by the following formula:

$$\text{Porosity} = \frac{\frac{w_s - w_m}{\rho_b}}{\frac{w_s - w_m}{\rho_b} + \frac{w_m}{\rho_m}} \times 100\%$$

where w_m and w_s are weights of the dry membrane and the membrane soaked in 2-propanol for 1h, respectively. ρ_b and ρ_m are the density of 2-propanol and dry membrane, respectively. Similarly, electrolyte uptakes of membranes were calculated by the following formula:

$$\text{Electrolyte uptake} = \frac{(w_e - w_m)}{w_m} \times 100\%$$

where w_e is weight of the membrane soaked in the liquid electrolyte for 2 h.

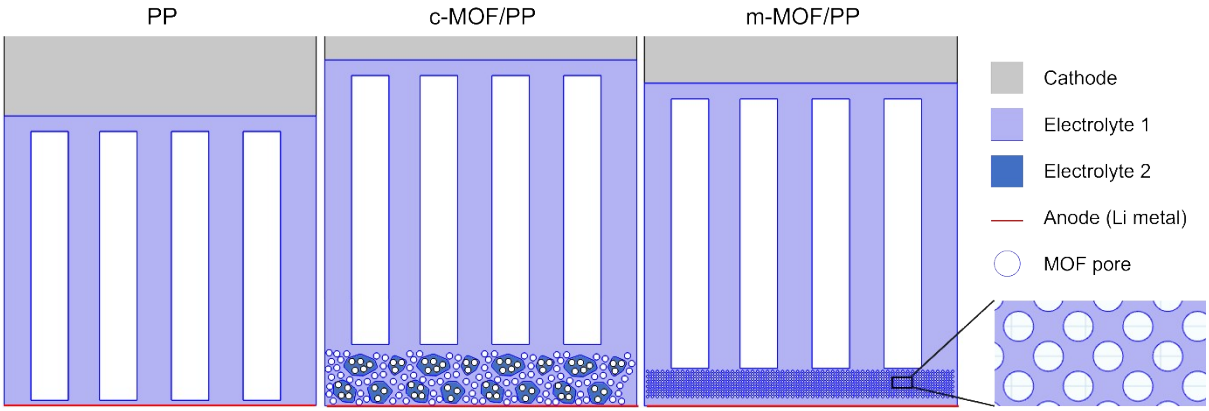

Fig. S1 Geometries of LMBs for the electrochemical simulations.

Table S1 Parameters used for 2D electrochemical modeling.

Parameter	PP	c-MOF/PP	m-MOF/PP
i_l (mA cm^{-2})	3	3	3
σ_l (S cm^{-1})	1×10^{-3}	1×10^{-3} (bulk), 1×10^{-7} (binder)	1×10^{-3}
Li^+ transference number (t_{Li^+})	0.25	0.25	0.25
c_l (mol L^{-1})	1	1	1
$i_{0,ref}$ (A m^{-2})	100	100	100
α_a	0.5	0.5	0.5

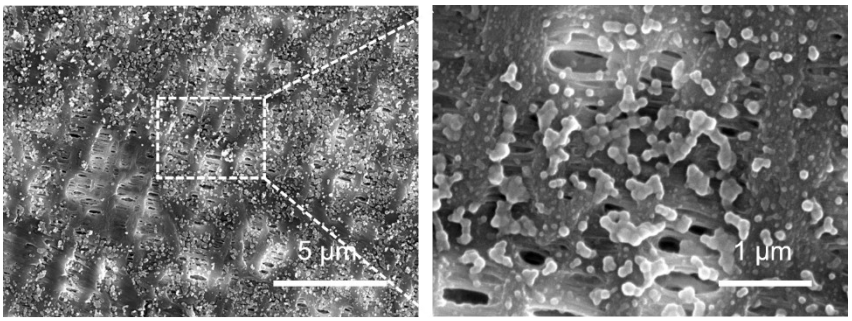

Fig. S2 SEM images of the m-MOF/PP after nucleation, confirming that the rhombic dodecahedral structure of ZIF-8 is not formed.

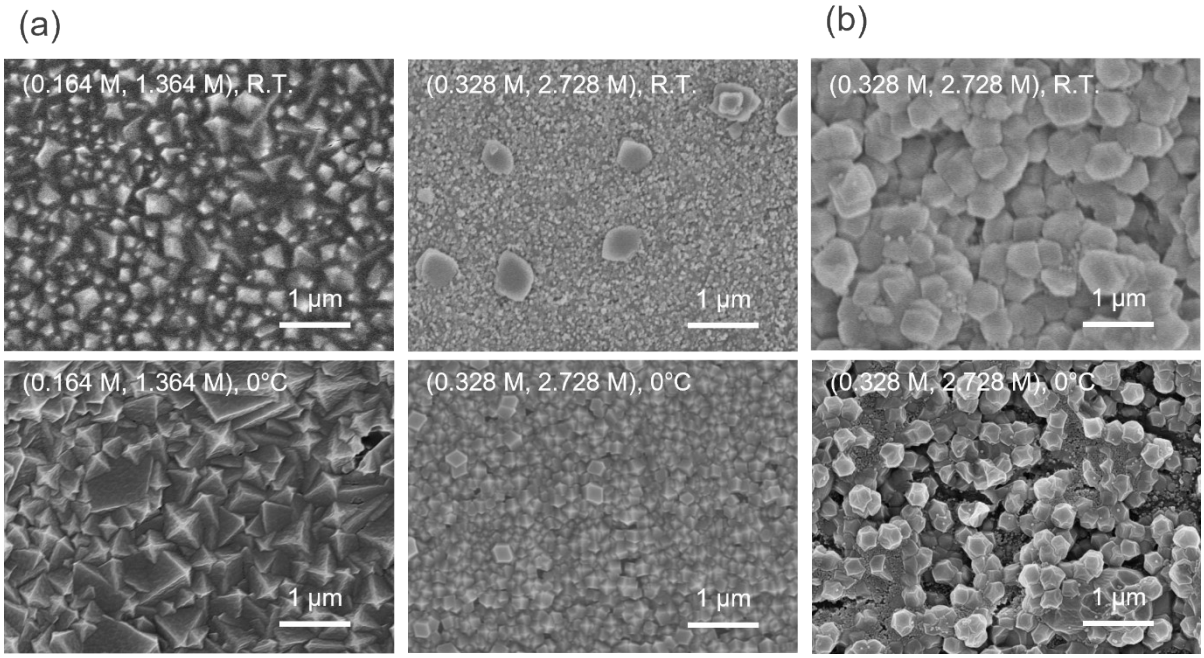

Fig. S3 SEM images of the m-MOF/PP synthesized under different conditions, such as types and concentrations of precursors and the temperature for the growth process. The precursors are (a) zinc acetate dihydrate, 2-methyl imidazole, and (b) zinc nitrate hexahydrate, 2-methyl imidazole. The concentration of precursors is shown in each image, as follows (Zn metal precursor, 2-methylimidazole). When using the zinc acetate dihydrate as Zn source, small well-defined cubic crystals of MOF are formed due to a high nucleation rate for zinc acetate precursor.[S1] A high concentration of precursors leads to equilibria shifting toward enhanced metal-ligand complexation thereby stopping crystal growth, resulting in small particles.[S1] The decrease in temperature of synthesis process induces the particles exhibiting higher purity and perfection.[S2]

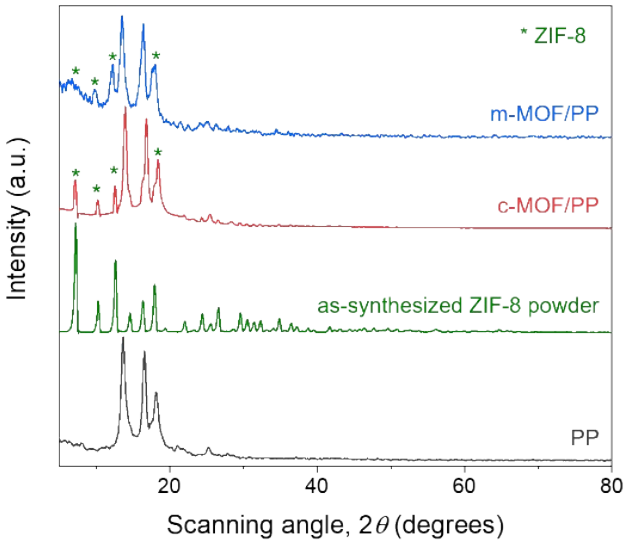

Fig. S4 XRD patterns of the m-MOF/PP, c-MOF/PP, MOF particle and PP.

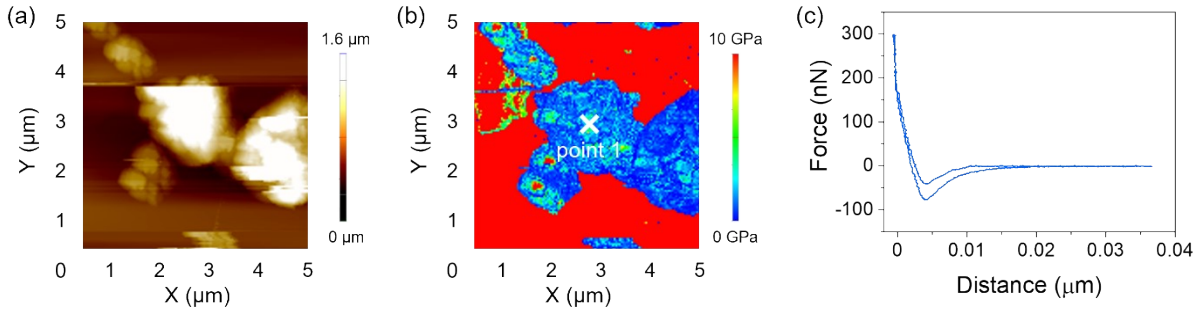

Fig. S5 (a) Topology and (b) distribution of *E* value of MOF particle on Si wafer, (c) FD curve of MOF particle at point 1, acquired using AFM.

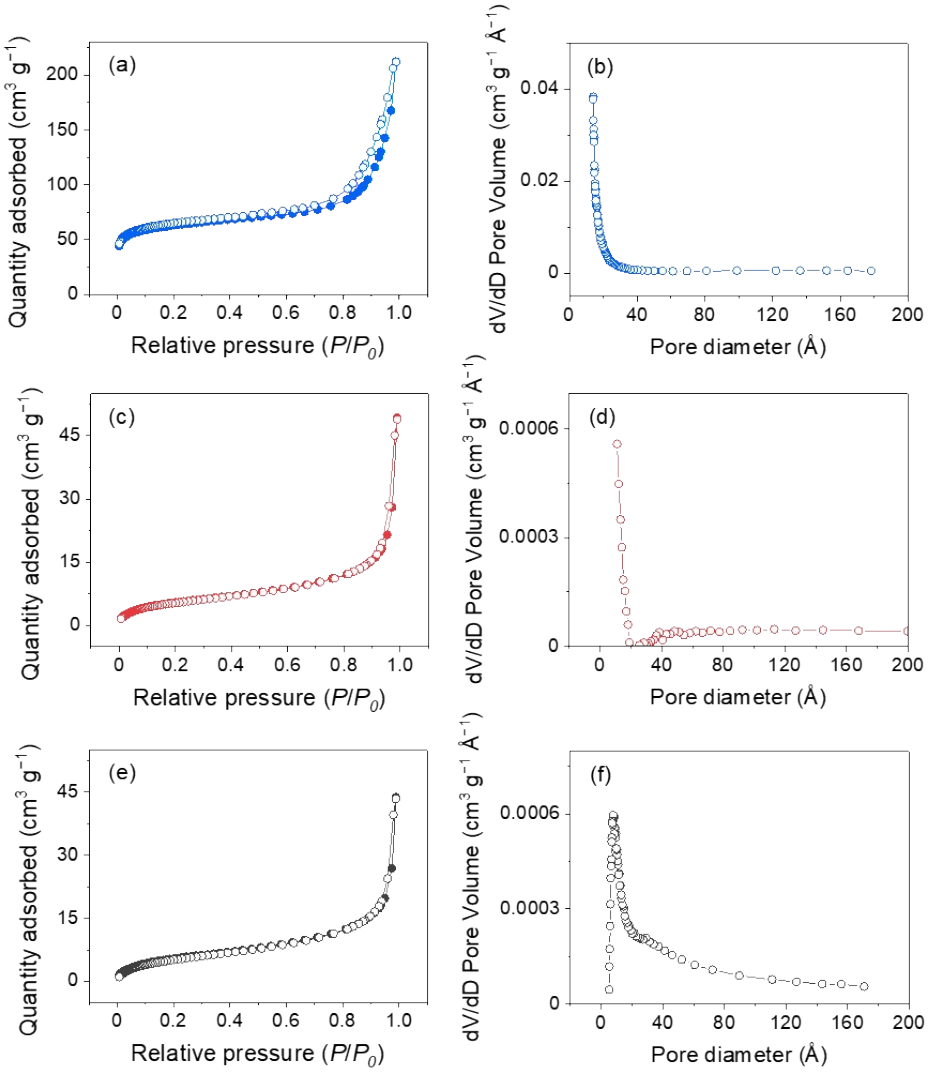

Fig. S6 (a, c, e) N_2 adsorption–desorption isotherm and (b, d, f) pore size distribution of (a, b) the m-MOF/PP, (c, d) the c-MOF/PP, and (e, f) PP.

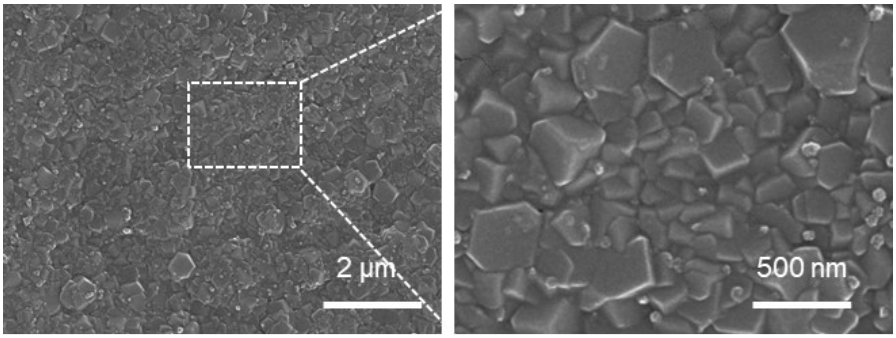

Fig. S7 FE-SEM images of m-MOF/PP membrane after electrolyte impregnation.

Separator	m-MOF/PP	c-MOF/PP	PP
SSIP (%)	34	40	89
CIP (%)	67	60	11

Table S2 Relative amounts of the SSIP and CIP in various membranes.

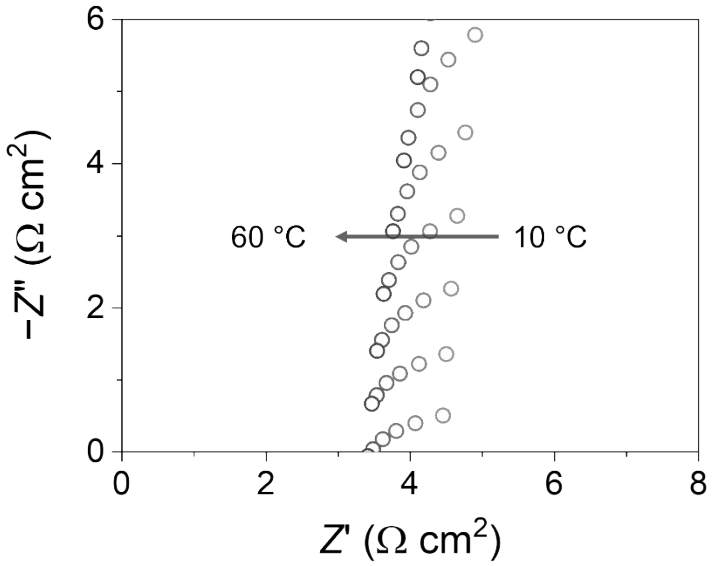

Fig. S8 AC-impedance spectra of electrolyte-impregnated PP at temperatures ranging from 10 to 60 °C.

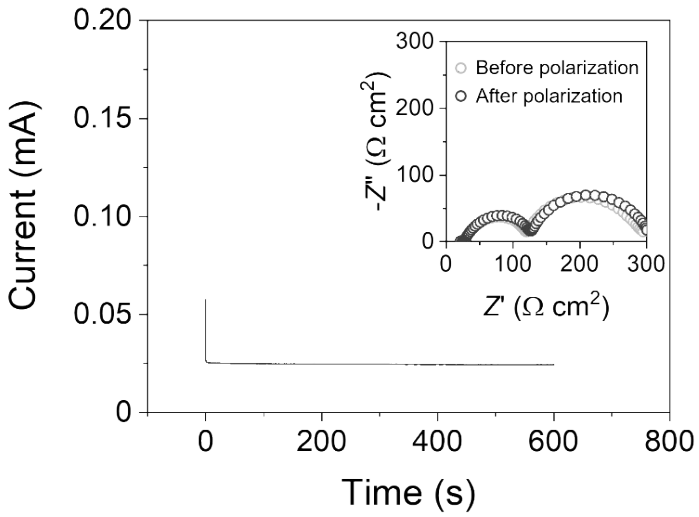

Fig. S9 DC polarization curve and AC-impedance spectra of electrolyte-impregnated PP.

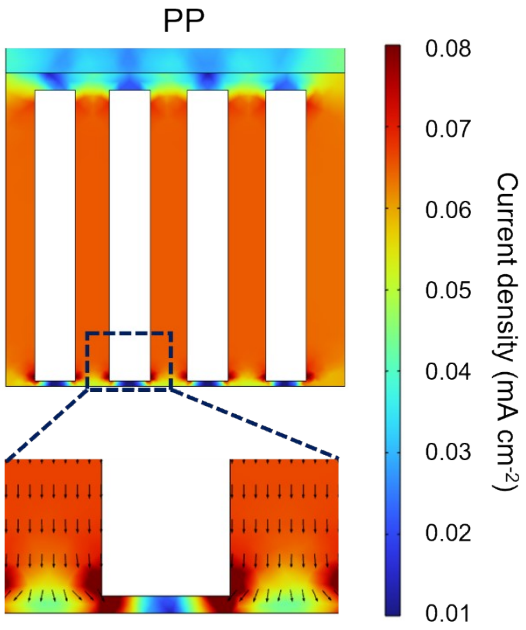

Fig. S10 Electrochemical modeling results for Li^+ flux and local current densities through PP.

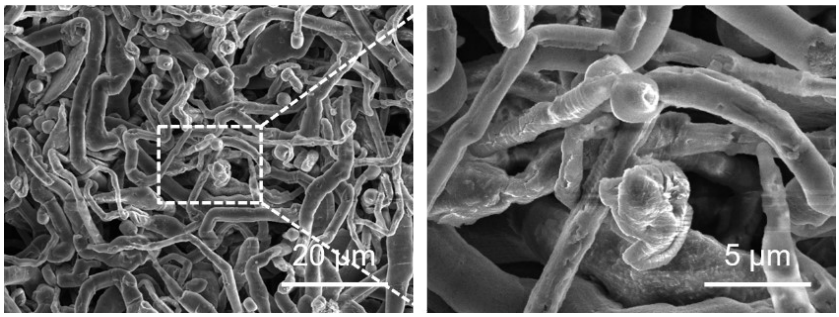

Fig. S11 SEM images of Cu substrate after Li deposition with a capacity of 10 mAh cm^{-2} at 1 mA cm^{-2} using [Li || Cu] cell with the PP.

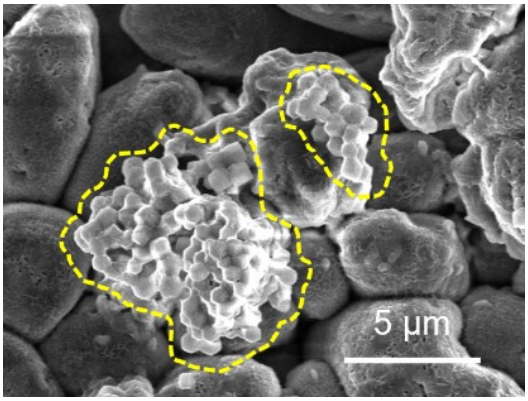

Fig. S12 SEM images of Cu substrate after Li deposition with a capacity of 10 mAh cm^{-2} at 1 mAh cm^{-2} using [Li || Cu] cell with the c-MOF/PP, showing the MOF particles exfoliated from the c-MOF/PP (inside the yellow dotted line).

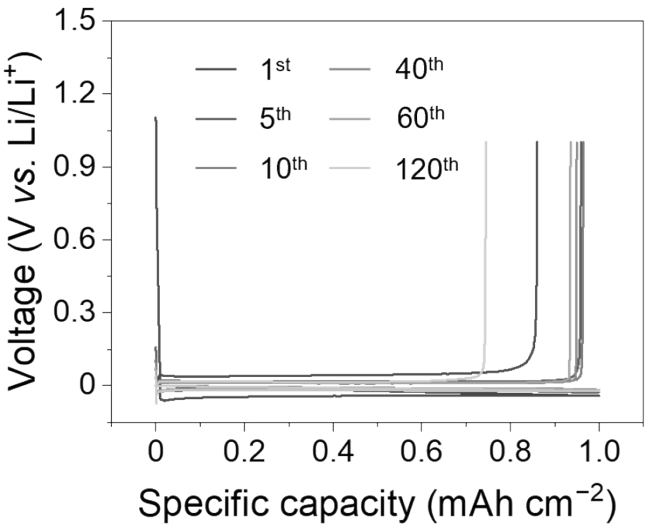

Fig. S13 Voltage profiles of [Li || Cu] cell with the PP measured during Li plating–stripping at 0.5 mA cm^{-2}.

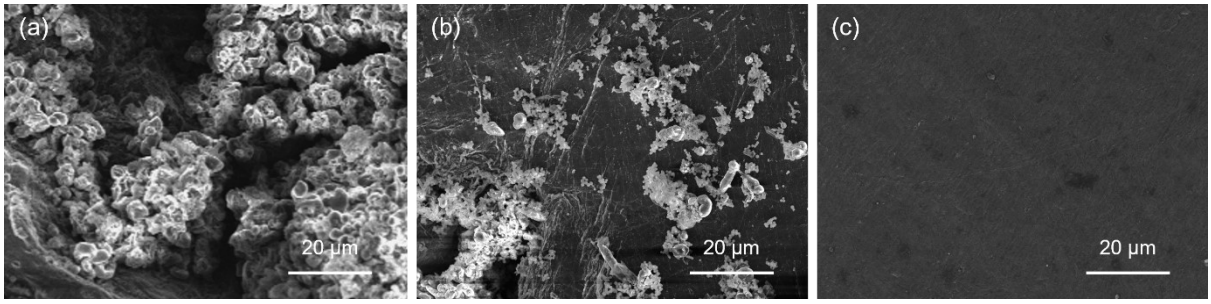

Fig. S14 Top view SEM images of Li anodes after 50 cycles using the [Li || Li] cells with the (a) PP, (b) c-MOF/PP and (c) m-MOF/PP.

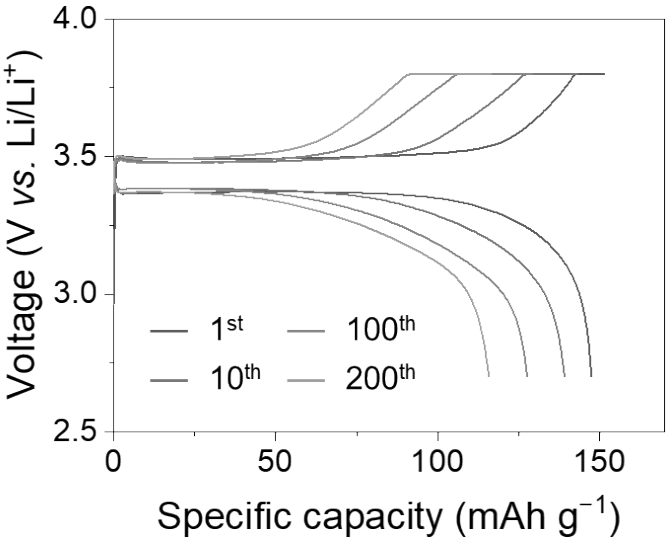

Fig. S15 Charge–discharge profiles of full cells with PP measured at 0.5C.

Table S3 Comparison of the electrochemical performances of the [Li || LFP] full cell using MOF-based membranes.

Membrane	Fabrication method	Test condition		Capacity retention	Ref.
		Electrolyte	C-rate		
PI-ZIF8	Slurry-casting	1 M $LiPF_6$ in EC/DMC/DEC /PEGDA/BMA	1C	75.2% after 300 cycles	[S3]
Hollow ZIF-8 membrane	Slurry-casting	1 M $LiPF_6$ in EC:DEC = 1:1 vol%	0.1C	85.1% after 100 cycles	[S4]
UIO-66/PAN/PVDF	Electrospinning	1 M $LiPF_6$ solution	1C	94.9% after 100 cycles	[S5]
3D-UIO-66/PAN	Electrospinning	LiTFSI-PEO ([EO]:LiTFSI = 18:1)	0.2C	86% after 300 cycles	[S6]
m-MOF/PP	Direct growth	1 M LiTFSI in DOL:DME = 1:1 with 1wt% $LiNO_3$	0.5C	96.6% after 300 cycles	This work

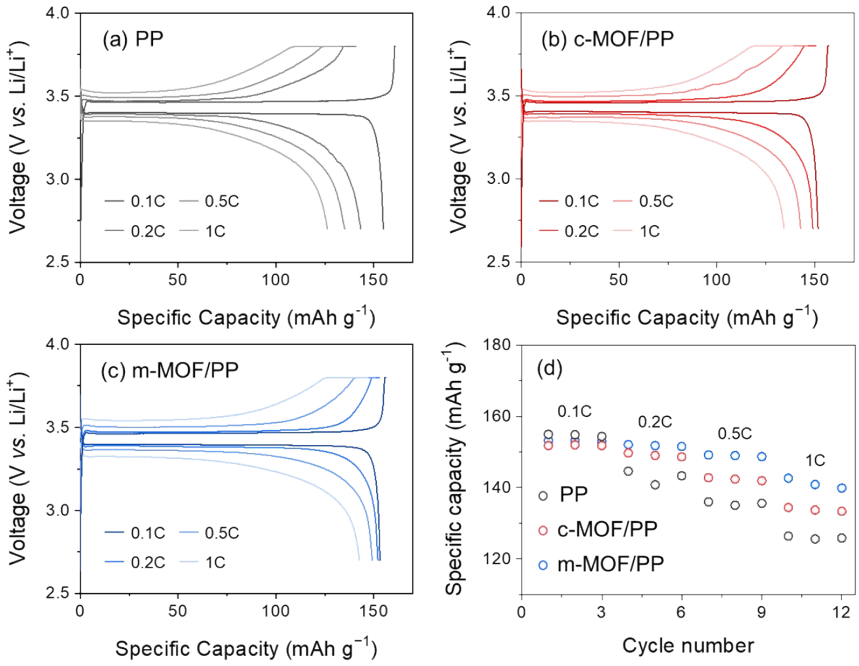

Fig. S16 Voltage profiles of the [Li || LFP] full cells using (a) PP, (b) c-MOF/PP, and (c) m-MOF/PP membrane operated at 0.1–1C. (d) Rate performances of the full cells using various membranes at 30 °C.

References

S1. A. G. Zavyalova, D. V. Kladko, I. Y. Chernyshov, V. V. Vinogradov, *J. Mater. Chem. A*, 2021, **9**, 25258.

S2. P. Chowdhury, C. Bikkina, D. Meister, F. Dreisbach, S. Gumma, *Microporous Mesoporous Mat.*, 2009, **117**, 406–413.

S3. G. Wang, P. He, L.-Z. Fan, *Adv. Funct. Mater*., 2021, **31**, 2007198.

S4. L. Tian, Z. Liu, ;F. Tao, M. Liu, Z. Liu, *Dalton Trans.*, 2021, **50**, 13877–13882.

S5. Q. Fu, W. Zhang, I. P. Muhammad, X. Chen, Y. Zeng, B. Wang, S. Zhang, *Microporous Mesoporous Mater.*, 2021, **311**, 110724.

S6. Z. Li, S. Wang, J. Shi, Y. Liu, S. Zheng, H. Zou, Y. Chen, W. Kuang, L. Chen, Y. Lan, Y. Cai, Q. Zheng, *Energy Storage Mater.*, 2022, **47**, 262–270.